Undercarboxylated, But Not Carboxylated, Osteocalcin Suppresses TNF-α–Induced Inflammatory Signaling Pathway in Myoblasts

Danbi Park,[1] Do-Yeon Kim,[2] Mi Ran Byun,[3] Hyorin Hwang,[1] Seong-Hee Ko,[1] Jeong-Hwa Baek,[4] and Kyunghwa Baek[1]

[1]Department of Pharmacology, College of Dentistry and Research Institute of Oral Science, Gangneung-Wonju National University, Gangwondo 25457, Republic of Korea
[2]Department of Pharmacology, School of Dentistry, Kyungpook National University, Daegu 41940, Republic of Korea
[3]Department of Pharmacology, College of Pharmacy, Kyung Hee University, Seoul 02447, Republic of Korea
[4]Department of Molecular Genetics, School of Dentistry and Dental Research Institute, Seoul National University, Seoul 08826, Republic of Korea
Correspondence: Kyunghwa Baek, PhD, 7, Jukheon-gil, Gangneung-si, Gangwon-do 25457. College of Dentistry. Bldg.#1 Rm # 211, Republic of Korea. Email: kb2012@gwnu.ac.kr.

Abstract

Undercarboxylated osteocalcin (ucOCN) has been considered to be an important endocrine factor, especially to regulate bone and energy metabolism. Even with the mounting evidence showing the consistent inverse correlation of ucOCN levels in chronic inflammatory diseases, however, the mechanism underlying the involvement of ucOCN in the muscular inflammation has not been fully understood. In the present study, we explored 1) the endocrine role of ucOCN in the regulation of inflammation in C2C12 myoblasts and primary myoblasts and the underlying intracellular signaling mechanisms, and 2) whether G protein–coupled receptor family C group 6 member A (GPRC6A) is the ucOCN-sensing receptor associated with the ucOCN-mediated anti-inflammatory signaling pathway in myoblasts. ucOCN suppressed the tumor necrosis factor-α (TNF-α)–induced expressions of major inflammatory cytokines, including interleukin-1β (IL-1β) and inhibited the TNF-α–stimulated activities of transcription factors, including NF-κB, in C2C12 and primary myoblasts. Both knockdown and knockout of GPRC6A, by using siRNA or a CRISPR/CAS9 system, respectively, did not reverse the effect of ucOCN on IL-1β expression in myoblasts. Interestingly, TNF-α–induced IL-1β expression was inhibited by knockdown or deletion of GPRC6A itself, regardless of the ucOCN treatment. ucOCN was rapidly internalized into the cytoplasmic region via caveolae-mediated endocytosis, suggesting the presence of new target proteins in the cell membrane and/or in the cytoplasm for interaction with ucOCN in myoblasts. Taken together, these findings indicate that ucOCN suppresses the TNF-α–induced inflammatory signaling pathway in myoblasts. GPRC6A is not a sensing receptor associated with the ucOCN-mediated anti-inflammatory signaling pathway in myoblasts.

Key Words: undercarboxylated osteocalcin, C2C12, anti-inflammation, GPRC6A, sarcopenia, IL-1β

Abbreviations: ATF2, activating transcription factor 2; BSA, bovine serum albumin; cAMP, cyclic adenosine monophosphate; DAPI, 4′,6-diamidino-2-phenylindole; DMEM, Dulbecco's Modified Eagle Medium; FBS, fetal bovine serum; GPRC6A, G protein–coupled receptor family C group 6 member A; IL-1β, interleukin-1β; IL-6, interleukin-6; NFκB, nuclear factor kappa B; OCN, osteocalcin; PBS, phosphate-buffered saline; PCR, polymerase chain reaction; ROS, reactive oxygen species; siCON, nontargeting control small interfering RNA; siGPRC6A, small interfering RNA targeting GPRC6A; TNF-α, tumor necrosis factor-α; ucOCN, undercarboxylated osteocalcin.

Osteocalcin (OCN) is the most abundant noncollagenous protein primarily produced by osteoblasts; however, it is also produced in smaller amounts by odontoblasts or hypertrophic chondrocytes [1, 2]. Osteocalcin is a bone protein containing γ-carboxyglutamic acid (Gla) with a size of 5.6 kDa (46 and 49 amino acids in mouse and human, respectively). In osteoblasts, the carboxylation process involves the addition of a carboxyl group at glutamic acid (Glu) residues in positions 17, 21, and 24, which is completed with vitamin K-dependent posttranslational modifications [3]. With these 3 γ-carboxyglutamic acid residues, osteocalcin binds to hydroxyapatite crystals in the bone matrix via a disulfide bond formed between cysteine residues [4]. Osteocalcin containing one or more "not carboxylated" glutamic acid residues is

denoted as undercarboxylated osteocalcin (ucOCN) [5]. Approximately 40% to 60% of the total osteocalcin released into the circulation exists in either a partially or completely uncarboxylated form, which exhibits endocrine functions, including regulation of energy metabolism, fertilization, and cognitive functions [5-13].

Muscle wasting, defined as the loss of skeletal muscle tissue, occurs naturally under physiological conditions, such as aging [14]. Muscle wasting is a feature associated with chronic wasting syndromes, such as AIDS, cancer, and diabetes, and neuroinflammatory disorders such as amyotrophic lateral sclerosis [15]. It is an independent predictor of mortality. In many such conditions, muscle wasting is associated with variable degrees of local and/or systemic chronic

inflammation, in particular, chronic elevations in circulating inflammatory cytokines, including tumor necrosis factor (TNF)-α [16-19]. Elevated levels of inflammatory mediators are known to trigger muscle wasting events. Carnio et al demonstrated that chronic administration of TNF-α or interleukin-1β (IL-1β) resulted in weight loss due to skeletal muscle wasting in rats [20]. Studies using diabetic rat models have reported that muscle wasting is closely associated with increased expression of TNF-α, IL-1β, and IL-6 in skeletal muscle [21]. In a cross-sectional clinical study, sarcopenia in older adults is associated with increased levels of pro-inflammatory mediators [22, 23]. In vitro studies have demonstrated that inflammatory cytokines play a crucial role in the onset and development of muscle wasting. Ye J et al reported that TNF-α inhibited the expression of α-actin and myosin heavy chain in primary cultures of human myoblasts [24]. TNF-α administration depleted myosin heavy chain in the murine skeletal muscle cell line C2C12 and primary cultures of rat skeletal muscle [25].

Previous studies have demonstrated that serum osteocalcin levels decrease with obesity or diabetes, which are associated with chronic inflammation [26]. In addition, low serum levels of ucOCN have been reported in patients with bone-related inflammatory diseases such as rheumatoid arthritis, osteoporosis, and ankylosing spondylitis [27-30]. Inspired by the consistent inverse correlation of ucOCN levels in chronic inflammatory diseases, we hypothesized that ucOCN has another endocrine role in the regulation of inflammation.

G protein–coupled receptor family C group 6 member A (GPRC6A) was identified as the ucOCN-sensing receptor [31]. GPRC6A-mediated osteocalcin signaling has been demonstrated in various tissues, including adipose, pancreas, testes, and skeletal muscle [26, 32, 33]. To probe the structural basis of osteocalcin binding to GPRC6A, Pi et al performed computational modeling experiments [34]. Predictions based on the modeling demonstrated the docking of the C-terminal hexapeptide of osteocalcin to the extracellular side of the transmembrane domain of GPRC6A. Thereafter, GPRC6A-mediated osteocalcin signaling has been demonstrated in pancreatic β-cells [35] and pancreatic acinar cells [36]. In skeletal muscle, fat, and hepatic cells, GPRC6A-mediated osteocalcin signaling has also been proposed. Liu et al demonstrated that osteocalcin induces proliferation and promotes differentiation via the activation of the GPRC6A-ERK1/2 pathway in C2C12 myoblast cells [37]. White fat accumulation and glucose intolerance/insulin resistance were observed in GPRC6A$^{-/-}$ mice, but not in wild-type mice [26, 32, 38-42]. Hepatic steatosis, as well as an increase in triglycerides and a decrease in glycogen storage/cholesterol levels, were observed in GPRC6A$^{-/-}$ mice. Pi et al [43] and De Toni et al [44] reported on a GPRC6A-dependent osteocalcin signaling pathway in testicular Leydig cells.

This study aimed to investigate 1) the endocrine role of ucOCN in the regulation of inflammation in C2C12 myoblasts and explore the underlying intracellular signaling mechanisms; and 2) whether GPRC6A is the ucOCN-sensing receptor associated with the ucOCN-mediated anti-inflammatory signaling pathway in C2C12 myoblasts.

Materials and Methods

Cell Culture and Experimental Design

C2C12 cells were cultured in Dulbecco's Modified Eagle's Medium (DMEM) (Hyclone, MD, USA) supplemented with 10% fetal bovine serum (FBS), 100 U/mL penicillin, and 100 μg/mL streptomycin (Hyclone) at 37 °C in a humidified atmosphere containing 5% CO_2. The cells were pretreated for 30 minutes by adding mouse ucOCN (0.5, 5, or 50 ng/mL) (Bachem, CA, USA) to DMEM containing 5% FBS. Subsequently, the cells were incubated with TNF-α (10 ng/mL) (Peprotech, NJ, USA) for 8, 24, and 48 hours.

Primary myoblasts were prepared from 4 mice (C57BL/6) at 8 weeks of age, as previously published [45, 46]. Skeletal muscle from the hindlimbs was isolated for the preparation. Muscle tissue was torn gently into small but distinguishable pieces (approximately > 0.5 mm^2) with sterile scissors and transferred into a 50 mL tube with the remaining 2 mL of the collagenase-dispase-CaCl$_2$. Tissue was incubated at 37 °C up to 30 to 40 minutes, then moved by gently agitating the tube every 5 to 10 minutes. Two volumes of proliferation medium were added and cells were released from the muscle fiber by pipetting up and down several times. The muscle solution was filtered using a 70-μm cell strainer and the cells were centrifuged and resuspended. The primary myoblast cells were seeded in each well of collagen-coated 6-well plates and cultured in F-12 media (Ham's F-12 Nutrient Mix), 20% FBS (Gibco), 10% horse serum (Gibco) at 37 °C in a humidified atmosphere containing 5% CO_2. The 5×10^5 seeded cells were pretreated for 30 minutes by adding mouse ucOCN (0.5, 5, or 50 ng/mL) (Bachem, CA, USA) to F-12 media containing 2% FBS and 1% horse serum. Subsequently, the cells were incubated with TNF-α (10 ng/mL) (Peprotech, NJ, USA) for 8 hours.

Real-Time Polymerase Chain Reaction Analysis

Quantitative real-time polymerase chain reaction (PCR) was performed to evaluate mRNA expression. Total RNA was isolated using easy-BLUE RNA extraction reagents (iNtRON Biotechnology, Kyungki-Do, Korea) according to the manufacturer's instructions. Complementary DNA was synthesized from 2.5 μg of total RNA using the AccuPower RT-PreMix MasterMix (Bioneer, Daejeon, Korea) under the following conditions: 42 °C for 60 minutes and 94 °C for 5 minutes. The sequences were amplified with quantitative real-time PCR using a mixture of AccuPower 2X GreenStar PCR MasterMix (Bioneer) and primers and were detected using Step One Plus Real-Time PCR System (Thermo Fisher Scientific, MA, USA) and then analyzed. The sequences of PCR primers used for real-time PCR analysis are provided in supplementary data (Supplemental Table 1) [47]. The target gene expressions were normalized using GAPDH expression.

Western Blot Analysis

The cells were washed with phosphate-buffered saline (PBS) and scraped using PRO-PREP Protein Extraction Solution (iNtRON Biotechnology). The amount of each sample was measured using the Bradford reagent (Sigma-Aldrich) and by measuring absorbance at 540 nm using a microplate spectrophotometer (BioTek, VT, USA) based on bovine serum albumin (BSA). A standard curve was obtained based on the serial dilutions of BSA. Equal amounts of protein were subjected to SDS-PAGE and subsequently electro-transferred onto a nitrocellulose membrane. The membranes were washed with 1× Tris-buffered saline containing 0.1% Tween 20 (1× TBST). The membranes were blocked with 5% nonfat dry milk for 1 hour and incubated for 3 hours at 4 ℃ with 1:1000 diluted anti-IL-1β (SC-520125, Santa Cruz

Biotechnology, TX, USA, RRID:AB_629741), anti-IL-6 (SC-130326, Santa Cruz Biotechnology, RRID:AB_2127596), anti-ERK (9102S,Cell Signaling Technology, MA, USA, RRID:AB_330744), anti-phospho-ERK (9101S, Cell Signaling Technology, RRID:AB_331646), anti-JNK (9252S, Cell Signaling Technology, RRID:AB_2250373), anti-phospho-JNK (9251S, Cell Signaling Technology, RRID:AB_331659), anti-p38 MAPK (9212S, Cell Signaling Technology, RRID:AB_330713), anti-phospho-p38 MAPK (9211S, Cell Signaling Technology, RRID:AB_331641), anti-p65 NF-κB (SC-8008, Santa Cruz Biotechnology, RRID:AB_628017), and anti-phospho-p65 NF-κB (SC-136548, Santa Cruz Biotechnology, RRID:AB_10610391), anti-GPRC6A (SC-67302, Santa Cruz Biotechnology, RRID:AB_2114007), anti-Elk-1 (9182S, Cell Signaling Technology, RRID:AB_2277936), anti-phospho-Elk-1 (9186S, Cell Signaling Technology, RRID:AB_2277933), anti-c-Jun (SC-166540, Santa Cruz Biotechnology, RRID:AB_2280720), anti-phospho-c-Jun (3270S, Cell Signaling Technology, RRID:AB_2129575), anti-ATF2 (35031S, Cell Signaling Technology, RRID:AB_2799069), anti-phospho-ATF2 (SC-8398, Santa Cruz Biotechnology, RRID:AB_626709), or anti-β-actin-HRP (SC-8432, Santa Cruz Biotechnology, RRID:AB_6266030) antibodies. This was followed by incubation with horseradish peroxidase (HRP)-conjugated secondary antibody for 1 hour at room temperature. β-Actin was used as a loading control. The membranes were washed with 1× Tris-buffered saline containing 0.1% Tween 20. Protein bands were visualized using Luminata Forte (Millipore, MA, USA) and detected with a ChemiDoc (Bio-Rad, CA, USA). The reproducibility of the results was confirmed after repeating at least 3 times, and the results of 1 experiment are presented.

Cell Fractionation

Cytoplasmic membrane and nuclear fractions were separated and extracted using a subcellular protein fractionation kit for cultured cells (Thermo Fisher Scientific) according to the manufacturer's instructions. The same amount of protein extracted from each site was analyzed by Western blot using an anti-ucOCN antibody (Enzo Life Sciences, NY, USA, RRID:AB_2064899).

To analyze the anti-Ikkα/β (SC-166231, Santa Cruz Biotechnology, RRID:AB_2260487), anti-phospho-Ikkα/β (2694S, Cell Signaling Technology, RRID:AB_2122296), anti-IκB (9242S, Cell Signaling Technology, RRID:AB_331623), anti-phospho-IκB (2859S, Cell Signaling Technology, RRID:AB_561111), anti-p65 NF-κB (SC-8008, Santa Cruz Biotechnology, RRID:AB_628017), and anti-phospho-p65 NF-κB (SC-136548, Santa Cruz Biotechnology, RRID:AB_10610391), cytoplasmic and nuclear fractions were extracted from the cells using the NE-PER nuclear and cytoplasmic extraction reagents (Thermo Fisher Scientific).

Detection of Intracellular Reactive Oxygen Species

C2C12 cells were seeded in 12-well culture plates at a density of 1×10^5 cells per well. After 24 hours, the cells were pretreated with 0.5 ng/mL ucOCN for 30 minutes and then treated with 10 ng/mL TNF-α. After 8 hours of exposure, CellROX Orange reagent (Invitrogen) was added to a final concentration of 5 μM for 30 minutes. Nuclear counterstaining was performed with NucBlue Live ReadyProbes reagent (Invitrogen), according to the manufacturer's instructions. The samples

were examined using an Axio Imager.A2 microscope (Zeiss, Oberkochen, Germany). Fluorescence signals were visualized with EVOS FL Auto Imaging System (Thermo Fisher Scientific).

Immunocytochemistry

C2C12 cells were grown on sterile cover glasses placed in 24-well culture plates and treated with 0.5 ng/mL of ucOCN for 0, 1, 5, 10 and 15 minutes. The cover glass was washed thrice with PBS and fixed with 3.7% formaldehyde for 15 minutes at room temperature. Cells were treated with PBS containing 0.1% Triton X-100 for 5 minutes. Nonspecific binding sites were blocked with 3% BSA in PBS for 1 hour at room temperature. The cells were incubated with an anti-ucOCN antibody (Enzo Life Sciences, RRID:AB_2064899) diluted 1:500 in 1% BSA for overnight at 4 °C. The cells were subsequently incubated for 90 minutes with an Alexa Fluor 488-conjugated goat anti-mouse IgG H&L antibody (Abcam, Cambridge, UK, RRID:AB_2576208) diluted 1:1000 in 1% BSA at room temperature. Cell nuclei were stained with 4′,6-diamidino-2-phenylindole (DAPI) solution (Enzo Life Sciences) and ucOCN-stained signal was analyzed by confocal microscopy. To identify the ucOCN endocytosis pathway, C2C12 cells were incubated with 200 μM genistein (caveolae-mediated endocytosis inhibitor) or 20 μM Pitstop2 (clathrin-mediated endocytosis inhibitor) for 15 minutes and then treated with 0.5 ng/mL ucOCN for 15 minutes. Immunocytochemical analysis was used for ucOCN localization. To confirm the colocalization of internalized ucOCN with caveola, C2C12 cells were grown on sterile cover glasses placed in 24-well culture dishes for 16 hours, washed with PBS, incubated with DMEM containing 0.1% FBS for 16 hours, and treated with 0.5 ng/mL of ucOCN for 15 minutes. Subcellular localization of ucOCN and Cav-1 (3267S, Cell Signaling Technology, RRID:AB_2275453) were analyzed by confocal microscopy.

RNA Interference of GPRC6A

siGENOME smartpool mouse GPRC6A siRNA and nontargeting control siRNA were purchased from Santa Cruz Biotechnology. C2C12 cells were transfected using Lipofectamine 2000 (Thermo Fisher Scientific) according to the manufacturer's instructions. C2C12 cells were transfected with siRNA targeting GPRC6A (siGPRC6A) or nontargeting control siRNA (siCON). C2C12 cells transfected with siCON or siGPRC6A were incubated with TNF-α (10 ng/mL) and/or ucOCN (0.5 ng/mL) for 8 hours.

GPRC6A Knockout by CRISPR/CAS9 System

To generate the plasmid containing a single guide RNA that targets the GPRC6A locus, a pair of oligos (5′-CACCGAAA CATCCATCGCGGTCTCA-3′ and 5′-AAACTGAGACCGC GATGGATGTTTC-3′) were annealed and then inserted into a BsmBI–digested lentiCRISPRv2 vector. The lentiCRISPRv2 was a gift from Feng Zhang (Addgene plasmid # 52961; http://n2t.net/addgene:52961; RRID: Addgene_52961) [48]. To generate GPRC6A-deficient C2C12 cells, the plasmid targeting GPRC6A was transfected into C2C12 cells by using Lipofectamine 3000 (Thermo Fisher Scientific) according to the manufacturer's instructions. To generate control cells, a lentiCRISPRv2 plasmid targeting GFP was introduced to the C2C12 cells. To select control and GPRC6A-deficient

C2C12 cells, 2 μg/mL puromycin was added at 48 hours posttransfection. GPRC6A deficiency was confirmed with immunoblotting.

Luciferase Reporter Assays

HEK 293 cells were seeded in a 96-well plate at a density of 1×10^4 cells/well and transiently transfected with the reporter plasmids using Lipofectamine 2000 (Thermo Fisher Scientific). During each transfection, 0.01 μg of the expression vector (p65 NF-κB or pGL3) and 0.01 μg Renilla luciferase plasmid were used as indicated. After 24 hours, the cells were harvested, and luciferase activity was measured using the Dual-Luciferase Reporter Assay System (Promega, WI, USA) according to the manufacturer's instructions. The relative luciferase activity was calculated after normalizing the transfection efficiency by Renilla luciferase activity.

Statistical Analysis

Statistical significance was determined using Student's *t* test. For the multiple comparisons, one-way ANOVA was performed. In those cases where a significant interaction ($P < 0.05$) was detected, the appropriate post hoc least significant difference (LSD) test was performed. Differences or changes were considered significant at $P < 0.05$. Data were analyzed by using the SAS program.

Results

ucOCN Mitigates the Expression of TNF-α–induced IL-1β in C2C12 Cells

To examine whether ucOCN regulates the expression of TNF-α-induced inflammatory factors, C2C12 cells were pretreated with ucOCN (0.5, 5, or 50 ng/mL) for 30 minutes, followed by treatment with TNF-α (10 ng/mL) for 8, 24, and 48 hours. C2C12 cells treated with TNF-α for 8, 24, and 48 hours demonstrated significantly increased IL-1β expression at both the mRNA and protein levels. TNF-α–induced IL-1β expression was significantly decreased upon treatment with 0.5, 5, and 50 ng/mL ucOCN at both the mRNA and protein levels (Fig. 1). At 24 hours, TNF-α–induced IL-1β expression was significantly increased by treatment with 50 ng/mL ucOCN temporarily; however, this increase was suppressed at 48 hours. In addition, the expression of IL-6, COX, and TNF-α was also analyzed. Although the level of expression and expression time point varies, ucOCN also demonstrated a downregulation of the expression of these genes (Supplemental Figure 1) [47]. The ucOCN treatment alone did not induce any regulating effect on IL-1β expression at 8 or 24 hours in C2C12 cells (Supplemental Figure 2) [47].

Subsequent experiments were conducted focusing on IL-1β, whose expression was most inhibited, and the expression inhibition was maintained consistently by ucOCN. These results suggest that ucOCN significantly mitigated the expression of TNF-α–induced inflammatory cytokines.

We also examined whether ucOCN regulates the expression of TNF-α–induced inflammatory factors in primary myoblasts. Primary Myoblasts were pretreated with ucOCN (0.5, 5, or 50 ng/mL) for 30 minutes, followed by treatment with TNF-α (10 ng/mL) for 8 hours. Primary myoblasts treated with TNF-α for 8 hours demonstrated significantly increased IL-1β expression at both the mRNA and protein levels. TNF-α–induced IL-1β expression was significantly decreased upon treatment with 0.5, 5, and 50 ng/mL ucOCN at both the mRNA and protein levels (Fig. 1J- 1K).

In addition, we compared the effect of carboxylated osteocalcin (OCN) and ucOCN on TNF-α induced IL-1β expressions in C2C12. The OCN did not exhibit regulatory effects on TNF-α–induced IL-1β expression in C2C12 (Supplemental Figure 3) [47].

ucOCN Inhibits the Phosphorylation of TNF-α–Mediated Transcription Factors in C2C12 Cells

We then explored whether the effect of ucOCN on proinflammatory cytokine expression was mediated via the inhibition of the nuclear factor kappa B (NFκB) pathway. In the canonical NFκB activation pathway, a cytoplasmic IKKα/β complex is phosphorylated, thereby leading to IκB phosphorylation and degradation and subsequent nuclear translocation of NFκB. TNF-α-stimulated C2C12 cells demonstrated enhanced phosphorylation of p65 NF-κB, which was markedly inhibited by treatment with ucOCN at 1, 10, and 30 minutes (Fig. 2A). TNF-α-stimulated primary myoblasts also demonstrated enhanced phosphorylation of p65 NF-κB, which was markedly inhibited by treatment with ucOCN (Supplemental Figure 4) [47]. In addition, the expression of phosphorylated p65 NF-κB increased by TNF-α stimulation in cytoplasmic and nuclear fractions was investigated during ucOCN treatment. TNF-α–stimulated C2C12 cells demonstrated nuclear translocation and the phosphorylation of p65 NFκB, which was markedly inhibited by treatment with ucOCN at 3 and 30 minutes (Fig. 2B). We used the luciferase reporter assay to investigate whether ucOCN treatment transactivates the p65 NF-κB promoter. The results showed that TNF-α–induced transcriptional activation of p65 NF-κB was blocked by a dose-dependent increase in ucOCN (Fig. 2C).

Additionally, the phosphorylation of ERK, p38 MAPK, and JNK, as well as the phosphorylation of Elk-1, ATF2, and c-Jun, which are pivotal mediators of the ERK, p38 MAPK, and JNK signaling pathways, respectively, were investigated. As shown in Fig. 3, among the MAPKs signaling pathways, p38 MAPK activation was the most prominently suppressed by ucOCN treatment (Fig. 3A-3C). The phosphorylation of p38 MAPK by TNF-α stimulation was reduced by ucOCN treatment at 1 and 10 minutes (Fig. 3B). ERK activation by ucOCN treatment was mostly observed only at 1 minute (Fig. 3A-3C). The phosphorylation of Elk-1, ATF2, and c-Jun transcription factors was also investigated (Supplemental Figure 5) [47]. The results of this study suggest that ucOCN downregulates IL-1β expression via the inhibition of the TNF-α–mediated downstream signaling pathway in C2C12 cells.

ucOCN Mitigates the TNF-α–Induced Production of Reactive Oxygen Species

TNF-α not only mediates the inflammatory response by regulating associated signaling pathways, including MAPK and NF-κB, but also functions as a regulator of the generation of reactive oxygen species (ROS), which may result in a vicious cycle, with aggravation of the inflammatory response. Thus, we investigated whether ucOCN regulates TNF-α–induced ROS production.

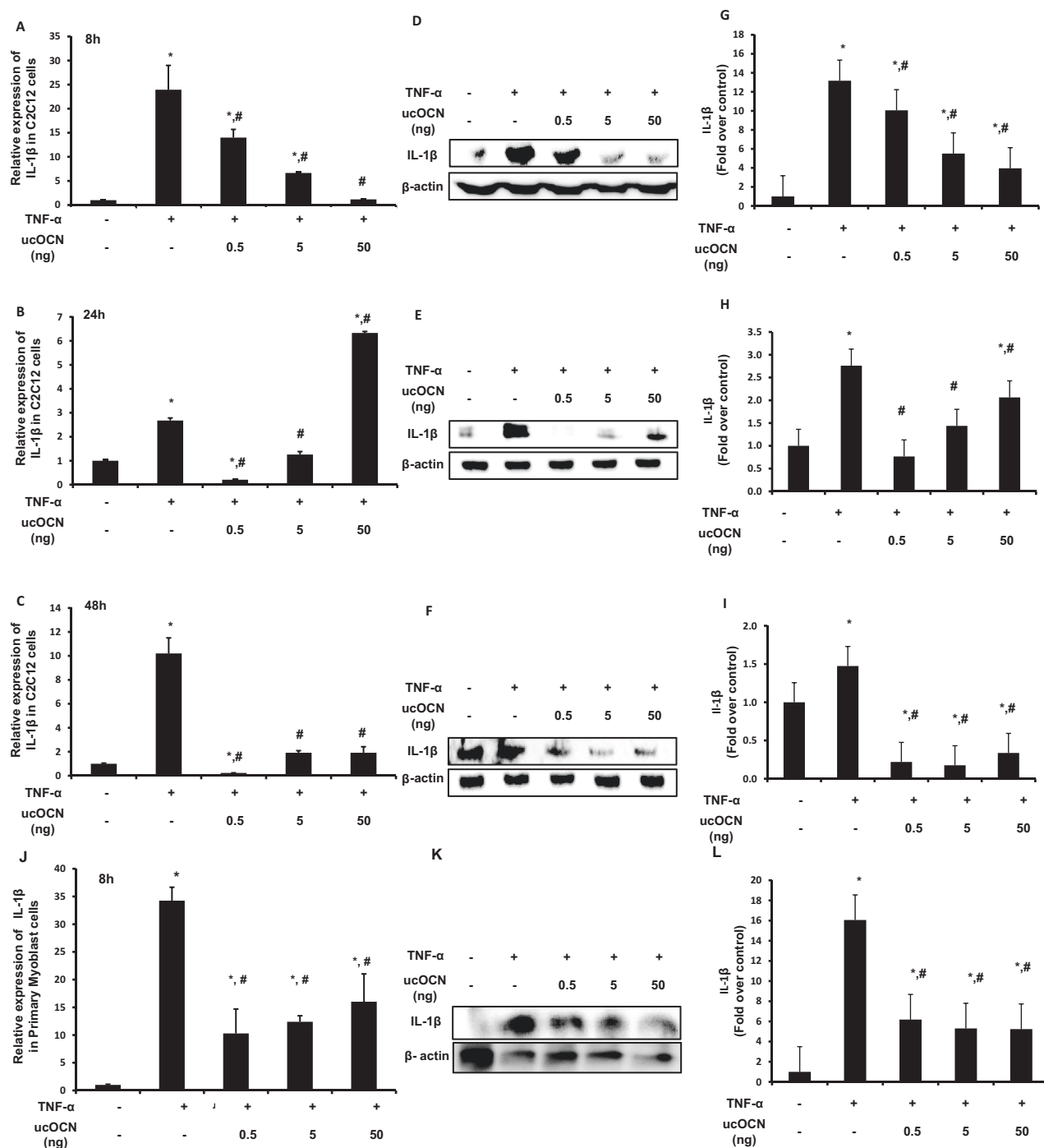As shown in Fig. 4, TNF-α treatment enhanced ROS production, which was inhibited by ucOCN (Fig. 4).

Figure 1. ucOCN mitigates the expression of TNF-α–induced IL-1β in C2C12 cells. C2C12 cells were pretreated with ucOCN (0.5, 5, or 50 ng/mL) for 30 minutes. The cells were then treated with TNF-α (10 ng/mL) for 8, 24, and 48 hours. The mRNA (A-C) and protein levels (D-F) of IL-1β were analyzed using real-time PCR and Western blot, respectively. (G-I) Quantification of the Western blot bands. (J-K) Primary myoblasts were pretreated with ucOCN (0.5, 5, or 50 ng/mL) for 30 minutes. The cells were then treated with TNF-α (10 ng/mL) for 8 and 48 hours. The mRNA (J) and protein levels (K) of IL-1β were analyzed using real-time PCR and Western blot, respectively. (L) Quantification of the Western blot bands. β-Actin was used as a loading control. Data represent the mean ± SD of triplicates. $*P < 0.05$ compared to CON; $^{#}P < 0.05$ compared to TNF-α.

GPRC6A Does Not Mediate ucOCN Signal in C2C12 Cells During the Regulation of Inflammation

Next, we performed experiments to verify a receptor transducing OCN signaling that mediates anti-inflammatory signaling in C2C12 cells. GPRC6A, a G-protein–coupled receptor, has been demonstrated as an osteocalcin-sensing receptor in various tissues [31-33, 49]. To determine whether

this receptor plays a role in myoblast cell biology, we first tested GPRC6A expression in C2C12 cells. As shown in Fig. 5A, GPRC6A is expressed in C2C12 cells. GPRC6A expression is relatively high in skeletal tissue [41]. To further verify the role of GPRC6A in mediating OCN signaling, we knocked down GPRC6A expression in C2C12 cells using siRNA. GPRC6A levels were efficiently reduced by GPRC6A-specific
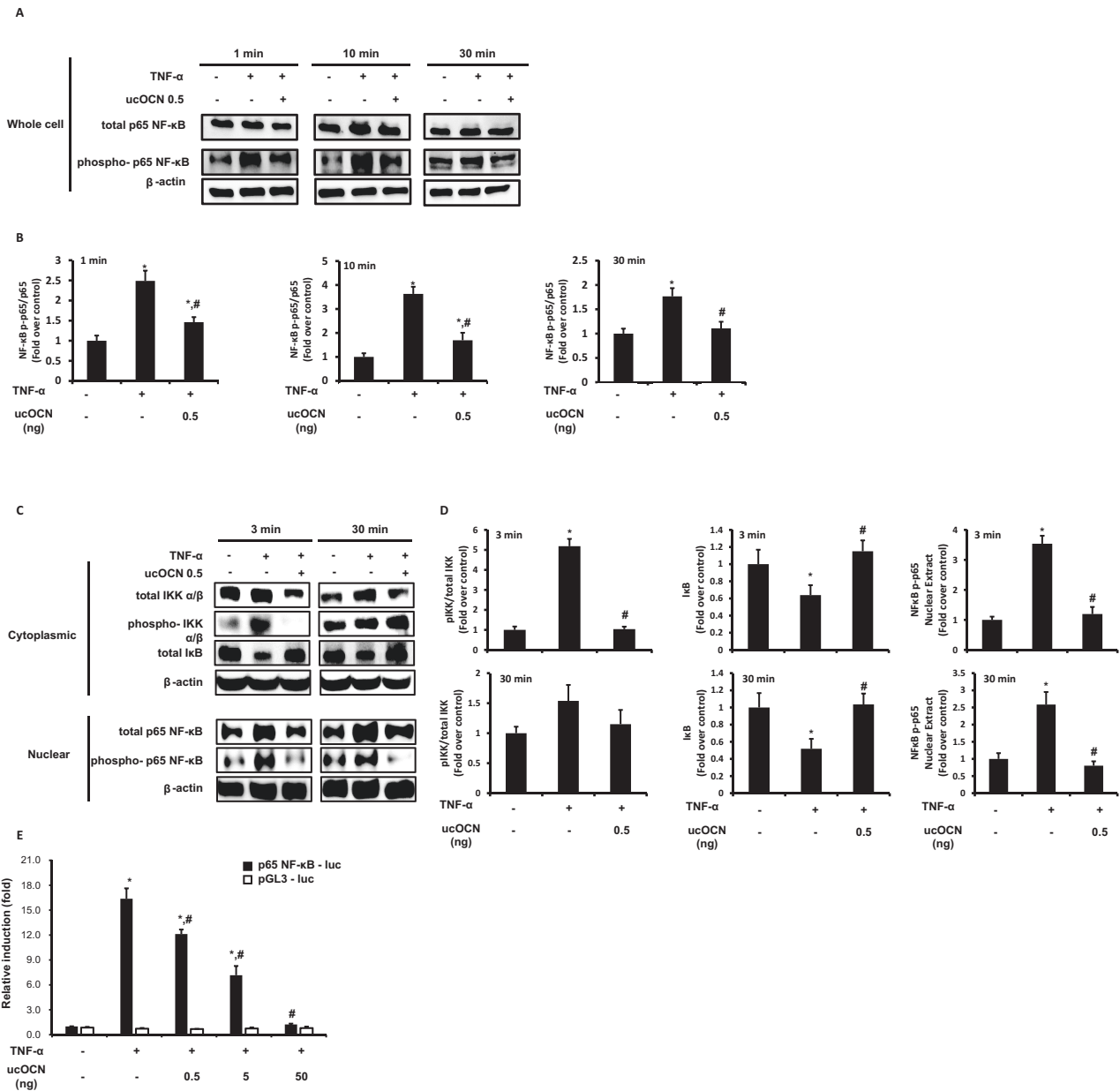
Figure 2. ucOCN inhibits the phosphorylation of TNF-α–mediated transcription factors. (A) C2C12 cells were treated with 10 ng/mL TNF-α and/or 0.5 ng/mL ucOCN for 1, 10 and 30 minutes. The extracted whole lysate was subjected to Western blot and analyzed using anti-p65 NF-κB antibody or anti-phospho-p65 NF-κB antibody. (B) Quantification of the Western blot bands. (C) C2C12 cells were treated with 10 ng/mL TNF-α and/or 0.5 ng/mL ucOCN. After 3 and 30 minutes, cytoplasmic and nuclear fraction lysates were extracted, and the expression of each antibody was analyzed using Western blot. (D) Quantification of the Western blot bands. (E) HEK 293 cells were transfected with pGL3 (control vector) or p65 NF-κB expression plasmids. After 24 hours, cells were treated with 10 ng/mL TNF-α and/or 0.5, 5, and 50 ng/mL ucOCN for 15 minutes. Subsequently, luciferase activity was measured. The resulting value is presented as firefly luciferase activity in comparison to the activity of Renilla. *$P < 0.05$ compared to p65 NF-κB-luc without TNF-α/ucOCN groups; #$P < 0.05$ compared to p65 NF-κB-luc with TNF-α groups.

siRNA. However, the knockdown of GPRC6A did not reverse the anti-inflammatory effect of ucOCN on IL-1β expression at either the mRNA or protein level (Fig. 5B and C).

CRISPR/CAS9-mediated deletion of GPRC6A in C2C12 showed the same result. We performed GPRC6A gene editing using the CRISPR/Cas9 system in order to knockout GPRC6A expression in C2C12 (Fig. 6A). To confirm the efficiency of intracellular GPRC6A receptor knockout, Western blot analysis was performed using an anti-GPRC6A antibody (Fig. 6B). The deletion of GPRC6A did not reverse the anti-inflammatory effect of ucOCN on IL-1β expression at either the

mRNA or protein level (Fig. 6C). These data suggest that the GPRC6A receptor does not transduce the OCN signal during inflammatory signaling in C2C12 cells (Fig. 6A). Interestingly, GPRC6A itself seemed to regulate TNF-α–induced IL-1β expression, regardless of the treatment with ucOCN. TNF-α–induced IL-1β expression was inhibited by knockdown or deletion of GPRC6A itself (Figs. 5B-5C and 6C). The anti-inflammatory effect of ucOCN was not significantly affected by the presence of GPRC6A, as observed when comparing the results in GPRC knockdown only or knockout only group and GPRC knockdown or knockout with ucOCN
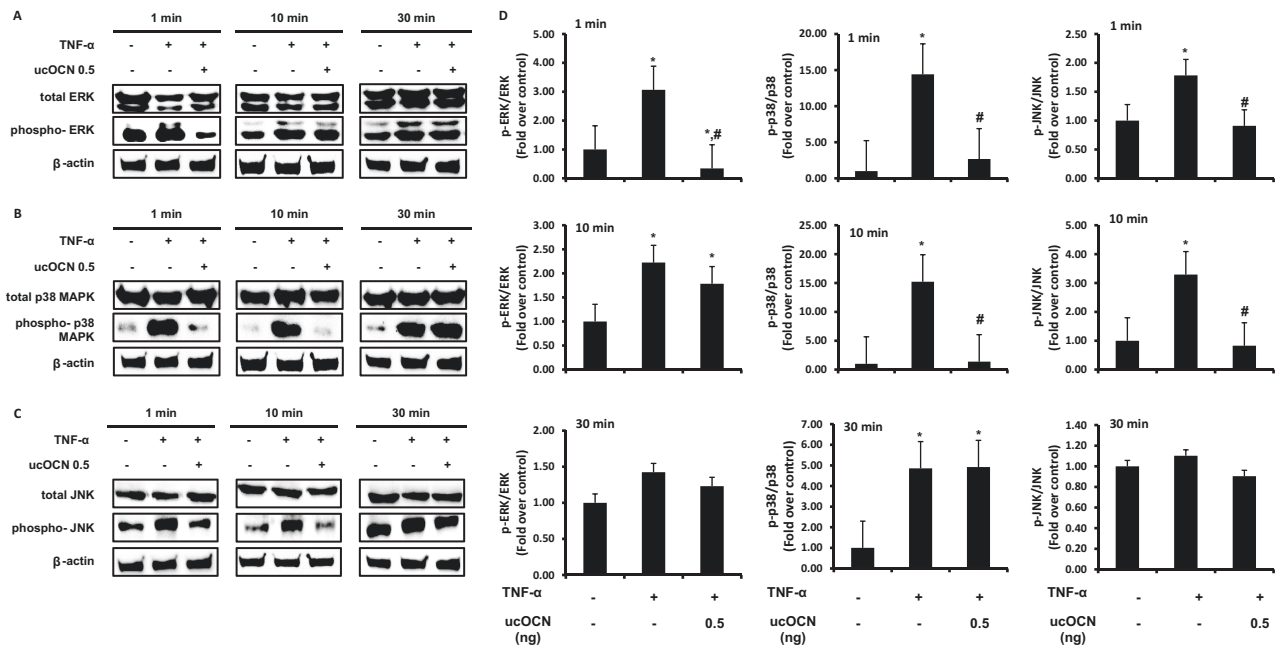
Figure 3. ucOCN inhibits the phosphorylation of TNF-α–mediated transcription factors. (A-C) C2C12 cells were treated with 10 ng/mL TNF-α and/or 0.5 ng/mL ucOCN for 1, 10, and 30 minutes. The extracted whole lysate was subjected to Western blot and analyzed using the anti-ERK antibody, anti-phospho-ERK antibody, anti-p38 MAPK antibody, anti-phospho-p38 MAPK antibody, anti-JNK antibody, or anti-phospho-JNK antibody. The blots were stripped and re-probed to visualize different proteins. (D) Quantification of the Western blot bands.

treatment group. Taken together, the GPRC6A receptor present in the C2C12 cells is not involved in the role of ucOCN-mediated inflammation regulation.

ucOCN Is Localized to the Cytoplasmic Region in C2C12 Cells

We investigated the subcellular localization of ucOCN protein over time in C2C12 cells using an anti-ucOCN antibody. As shown in Figs. 7A and 7B, ucOCN cytoplasmic localization started at 5 minutes after ucOCN treatment and was maintained by 15 minutes. Cells were incubated with genistein (caveolae-mediated endocytosis inhibitor) or Pitstop2 (clathrin-mediated endocytosis inhibitor) for 15 minutes to identify the ucOCN endocytosis pathway. As shown in Fig. 7C, Pitstop2 pretreated cells were localized inside the cytoplasm, which is the same as untreated cells. However, the ucOCN cytoplasmic localization was obviously inhibited by genistein. Colocalization of caveolae and ucOCN were observed under the stimulation of ucOCN treatment (Fig. 7D).

These results suggest that ucOCN was internalized and acted as an anti-inflammatory regulator when present in the cytoplasmic region. In addition, data indicate that ucOCN cytoplasmic localization is involved with caveolae-mediated endocytosis and is independent of the clathrin-mediated endocytic pathway.

Discussion

Our primary hypotheses that undercarboxylated osteocalcin (ucOCN) suppresses TNF-α-induced inflammatory responses and that GPRC6A mediates this inflammation regulatory function of ucOCN were set based on the following reasoning: 1) several clinical and animal studies show an inverse relationship between the serum level of ucOCN and chronic inflammation [26-30, 50, 51]; 2) GPRC6A is mainly expressed in myocytes; and 3) GPRC6A-mediated ucOCN signaling has been demonstrated in skeletal muscles as well as adipose, pancreas, and testes [52-54]

We demonstrated that ucOCN inhibits TNF-α–induced expression of pro-inflammatory cytokines, including IL-1β, in an NFκB-and MAPK-dependent manner in myoblasts. Our data revealed that GPRC6A is not the receptor that transduces OCN signaling that mediates anti-inflammatory signaling in C2C12 cells. To our knowledge, this is the first study to demonstrate the regulatory role of osteocalcin in the inflammatory response in myoblastic cells and investigating the sensing receptor that transduces OCN signaling during inflammatory signaling in C2C12 cells.

In the present study, we explored the intracellular anti-inflammatory signaling mechanisms of ucOCN in TNF-α-stimulated C2C12 cells. ucOCN suppressed the activities of multiple TNF-α-stimulated transcriptional effectors, including NF-κB and MAPKs such as p38.

In C2C12 cells, TNF-α–induced increase in IL-1β expression was significantly mitigated by ucOCN (Fig. 1). Upon stimulation by inflammatory cytokines such as TNF-α, the NF-κB signaling pathway is activated [55]. Therefore, as a result of confirming the p65 NF-κB pathway in the cytoplasmic and nuclear site, it was determined that ucOCN inhibits nuclear translocation of p65 NF-κB (Fig. 2). Elk-1 is a downstream transcription factor that is activated by ERK-dependent phosphorylation and causes transcriptional activation of target genes in the nucleus [56]. p38 MAPK activates its downstream effector, the activating transcription factor 2 (ATF2). ATF2 transcriptional activity can be regulated in response to various stimuli, such as genotoxic agents, serum, and ionizing radiation, via phosphorylation of Thr69 and Thr71 residues by p38 MAPK and JNK [57, 58]. Activation of JNK induces the phosphorylation of c-Jun at residues Ser63 and Ser73 and inhibits ubiquitination and
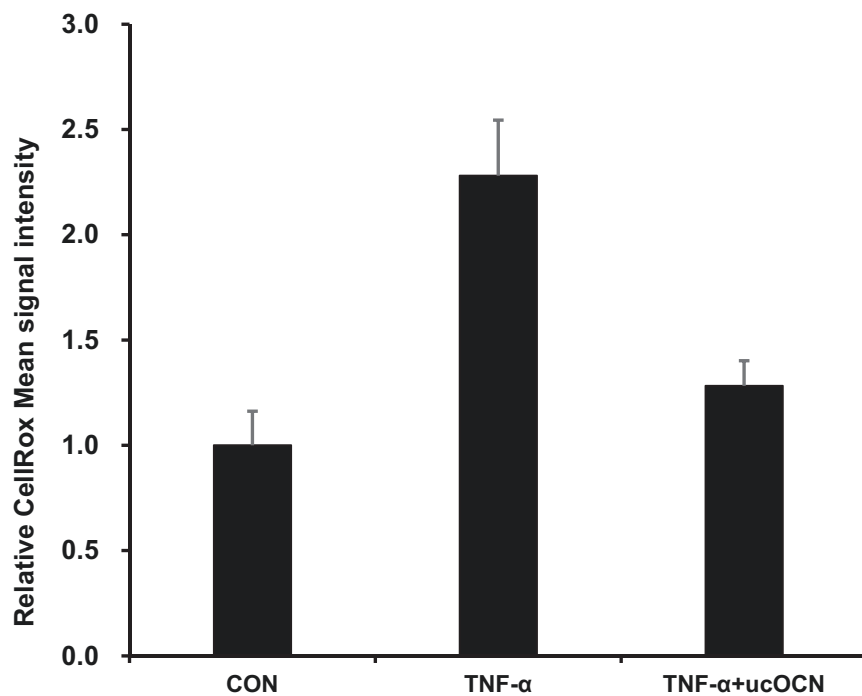
A
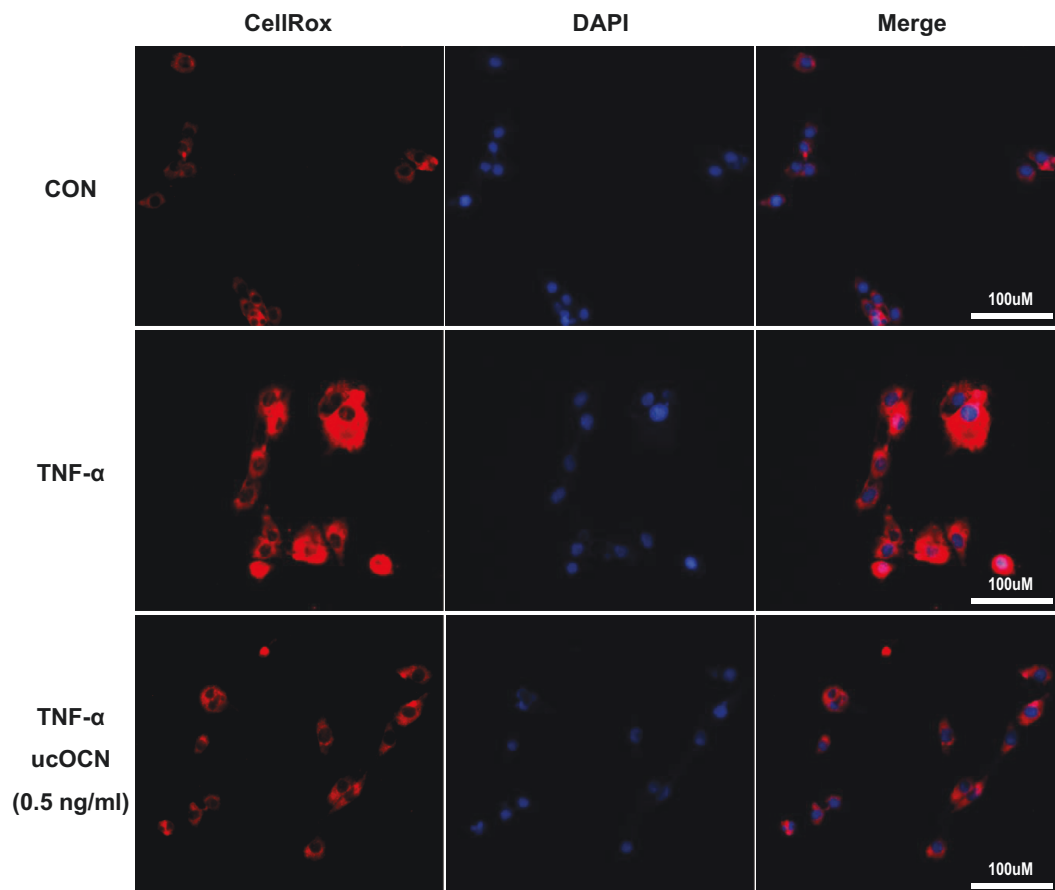
B

Figure 4. ucOCN mitigates the TNF-α-induced production of reactive oxygen species (ROS). (A) Measurement and (B) quantification of intracellular ROS levels with CellROX Orange staining. Cells were treated with 10 ng/mL TNF-α for 8 hours, with (lower panels) or without (middle panels) pretreatment with 0.5 ng/mL ucOCN for 30 minutes. Untreated control cells are shown in the upper panels. Nuclear staining is shown in blue. Scale bar 100 μm.
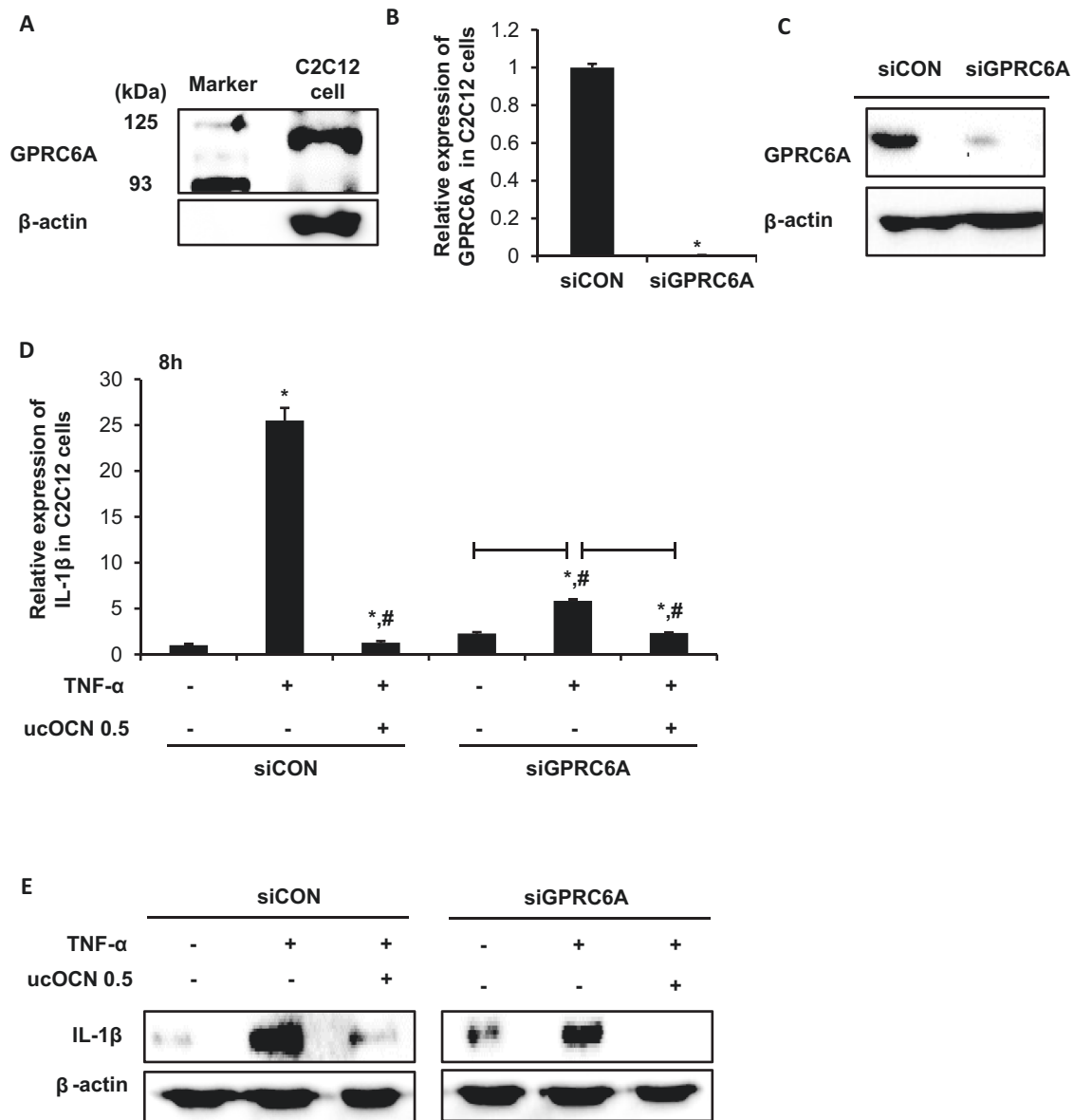
Figure 5. GPRC6A knockdown does not restore ucOCN-mediated IL-1β downregulation. (A) Western blot analysis was performed to determine the expression of GPRC6A using the whole lysate in C2C12 cells. (B, C) The C2C12 cells were transfected with nontargeting control siRNA (siCON) or siRNA targeting Gprc6a (siGPRC6A). The efficiency of GPRC6A knockdown was confirmed by quantitative RT-PCR and Western blot analysis. (D-E) C2C12 cells transfected with siCON or siGPRC6A were incubated with TNF-α (10 ng/mL) and/or ucOCN (0.5 ng/mL) for 8 hours. The effect of GPRC6A knockdown on mRNA and protein levels corresponding to IL-1β was analyzed using quantitative real-time PCR and Western blot, respectively. The data represent the mean ± SD of triplicates. *$P < 0.05$ compared to siCON-transfected cells without treatment; #$P < 0.05$ compared to siCON-transfected cells with TNF-α treatment; Brackets show a significant difference ($P < 0.05$) between indicated groups.

degradation of c-Jun [59-62]. As shown in Fig. 3, ucOCN blocked ERK, MAPK, and JNK phosphorylation: among the MAPK signaling pathways, p38 MAPK activation was most prominently suppressed by ucOCN treatment (Fig 3). ucOCN also blocked the phosphorylation of Elk-1, ATF2, and c-Jun that mediate their anti-inflammatory effects. Although the ERK, p38, JNK, and NF-κB signals were partially regulated by ucOCN, further studies are needed to determine the time difference required for the regulation of each inflammatory factor or the degree of suppression.

Accumulating studies have demonstrated the osteocalcin signaling pathway and its transcriptional effector in various cell types. Zhou et al reported the p65-NFκB-dependent osteocalcin signaling pathway in vascular tissues,

demonstrating that osteocalcin reverses obesity-induced endoplasmic reticulum stress and autophagic dysfunction [63]. The ERK (Gq pathway)-dependent osteocalcin signaling pathway was implicated in a GPRC6A transfected HEK 293 study conducted by Pi et al [64]. In contrast, Jacobsen et al showed that osteocalcin does not induce the activation of the ERK signaling pathway or any of the other G-protein signaling pathways that were tested in the GPRC6A-transfected Chinese hamster ovary cell line [65]. The Karsenty group has reported that osteocalcin does not induce the activation of the ERK pathway in TM3 Leydig cells. Rather, they showed that osteocalcin leads to cyclic AMP (cAMP) accumulation (Gs coupling) in TM3 Leydig cells [66]. The Quarles group also reported that 4 GPRC6A
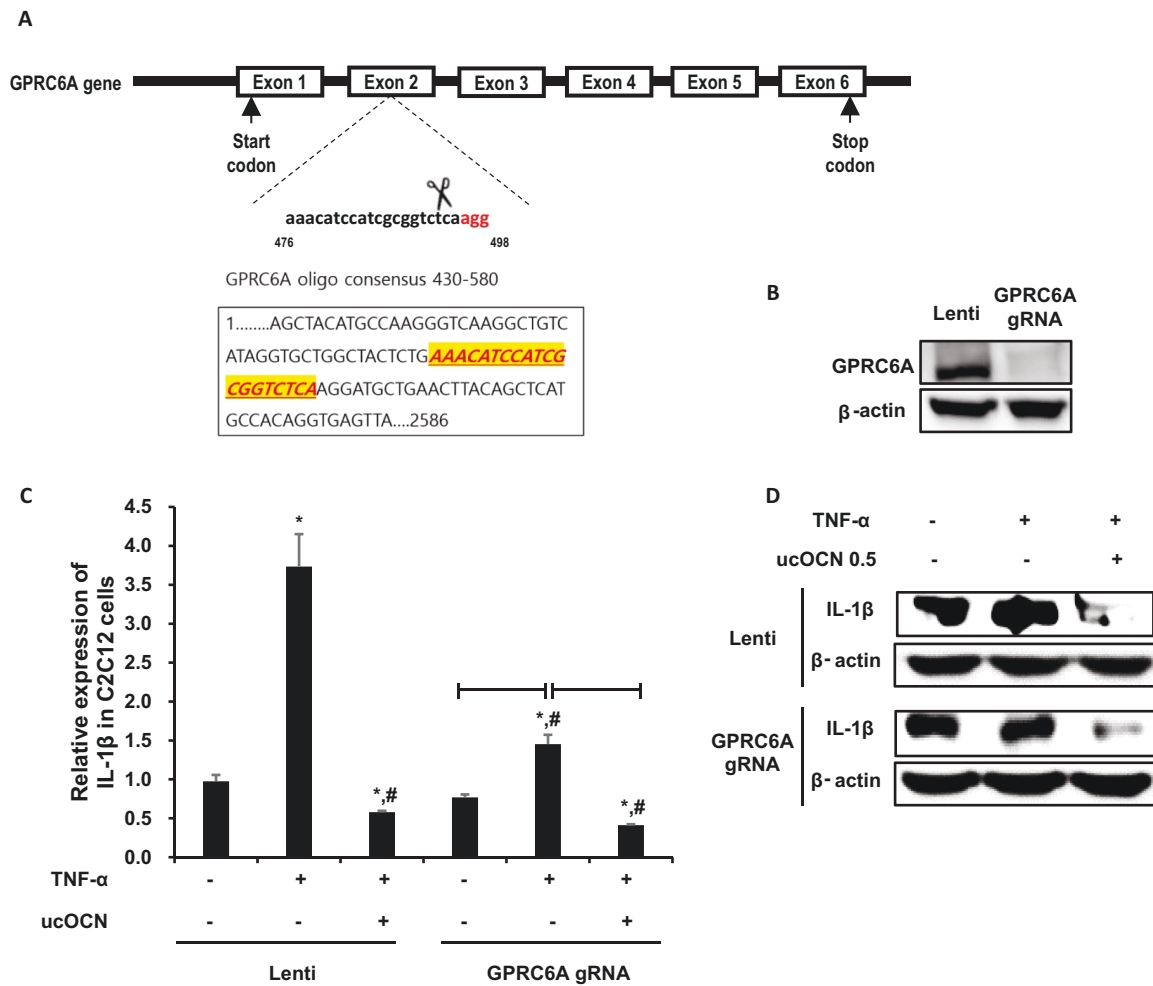
Figure 6. GPRC6A knockout does not restore ucOCN-mediated IL-1β downregulation. (A) Schematic illustration of the CRISPR/CAS9 system design. The highlighted bar shows the nucleotide sequences of the gRNA/cas9 (476-495). (B) The efficiency of CRISPR/Cas9-driven GPRC6A knockout was confirmed using Western blot. β-actin was used as a loading control. (C) After treatment with 10 ng/mL of TNF-α with or without ucOCN pretreatment, the effect of GPRC6A knockout on mRNA and protein levels corresponding to IL-1β was analyzed using quantitative real-time PCR and Western blot, respectively. The data represent the mean ± SD of triplicates. * $P < 0.05$ compared lentiCON-transfected cells without TNF-α treatment; #$P < 0.05$ compared to lentiCON-transfected cells with TNF-α treatment; Brackets show a significant difference ($P < 0.05$) between indicated groups.

agonists (osteocalcin, testosterone, L-arginine, and divalent cations) can induce G coupling by showing cAMP accumulation in GPRC6A-transfected HEK 293 cells [49, 67]. Our laboratory [36] demonstrated that ucOCN downregulates pancreatic lipase expression in a cAMP/PKA/ATF4- dependent pathway, indicating Gs coupling in pancreatic acinar cells. In myofibers, the CREB pathway has been reported as a mediator of osteocalcin signaling: CREB phosphorylation in myotubes is weaker after exercise, which was demonstrated using muscle-specific GPRC6A knockout mice [68]. In the present study, we demonstrated that ucOCN simultaneously remarkably inhibited the activities of TNF-α-stimulated multiple inflammatory regulators, including NF-κB, MAPKs such as JNK, p38, and ERK. Furthermore, ucOCN significantly suppressed ROS production, which implies that it may play a role in cellular antioxidant defense. These observations establish that osteoblasts and muscle cells are closely connected in various ways to regulate inflammatory reactions. Although ucOCN can exert effects on multiple pathways, the direct targets of ucOCN should be explored further in the future. In the present study, we explored the intracellular anti-inflammatory signaling mechanisms of OCN in conjunction with

the TNF-α-induced signaling pathway in C2C12 cells. Thus, further studies are also needed to explore the direct targets of ucOCN, regardless of TNF-α stimulation.

Interestingly, TNF-α–induced IL-1β expression was significantly increased by treatment with 50 ng/mL ucOCN temporarily at 24 hours; however, this increase was suppressed at 48 hours (Fig 1). We conducted this experiment several times to confirm the reproducibility and the aspect of high ucOCN (50 ng) regulation on lL-1β mRNA expression at 24 hours seemed somewhat inconsistent. In most of the data, TNF-α–induced IL-1β mRNA expression was significantly suppressed with ucOCN 50 ng treatment, as shown in 8-hour and 48-hour time points, but sometimes an expression increment (or no suppression) was observed (25% out of total experiment cases to test reproducibility). It is conjectured that high concentration (50 ng) ucOCN does show oscillation in regulating TNF-α–induced IL-1 β mRNA expression in C2C12 cells.

Our results showed that ucOCN suppressed TNF-α–induced pro-inflammatory cytokine expressions. However, both knockdown and knockout of GPRC6A receptor did not reverse the anti-inflammatory effect of ucOCN on IL-1β
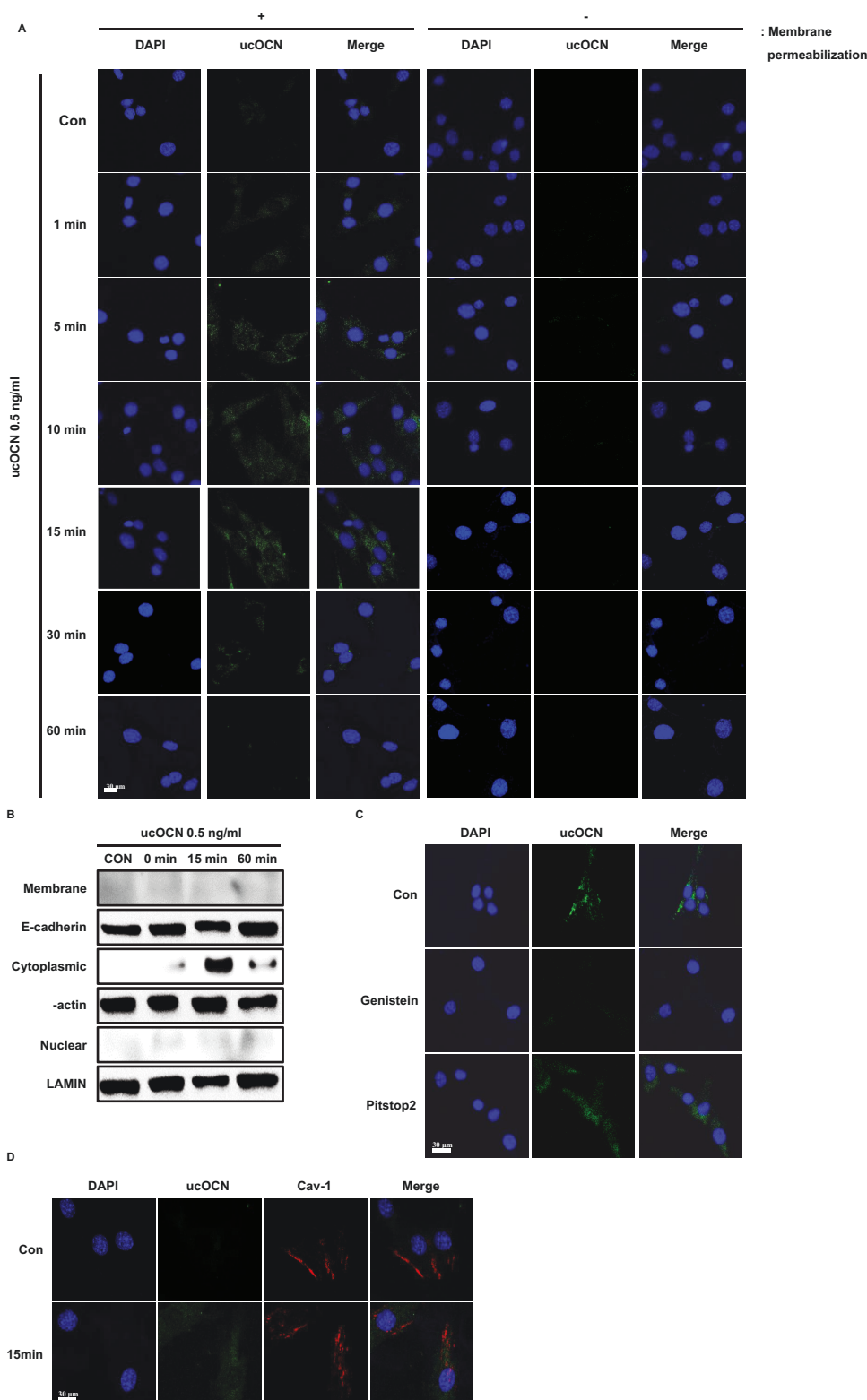
Figure 7. Time-dependent subcellular localization following ucOCN stimulation in C2C12 cells. (A) Time-dependent subcellular localization after ucOCN stimulation in C2C12 cells. C2C12 cells were grown on sterile cover glasses placed in 24-well culture dishes and stimulated with 0.5 ng/mL of ucOCN for the indicated times. Subcellular localization of ucOCN was confirmed using an anti-ucOCN antibody and an Alexa Fluor 488-conjugated goat anti-Mouse IgG H&L antibody. Cell nuclei were stained with DAPI solution (blue). (B) CON groups were treated with DMEM containing 10% FBS without ucOCN. Other groups were treated with 0.5 ng/mL ucOCN in DMEM containing 5% FBS for the indicated times. Proteins were extracted from cell membranes and the cytoplasmic and nuclear fractions. The extracted proteins were subjected to Western blot and analyzed using an anti-ucOCN antibody. (C) C2C12 cells were incubated with 200 μM Genistein (caveolae-mediated endocytosis inhibitor) or 20 μM Pitstop2 (clathrin-mediated endocytosis inhibitor) for 15 minutes and then treated with 0.5 ng/mL ucOCN for 15 minutes. ucOCN localization was analyzed by immunocytochemical analysis. Green fluorescence signal indicates ucOCN and DAPI staining was used as a nucleus counterstain. (D) Subcellular localization of ucOCN and Cav-1 (caveolin-1: caveolae-mediated endocytosis marker) were analyzed by confocal microscopy.

expression at either the mRNA or protein level, suggesting that the GPRC6A receptor present in the C2C12 cells is not involved in the role of ucOCN-induced inflammation regulation. In addition, as shown in Fig. 7, ucOCN localized to the cytoplasm in caveolae-mediated endocytic pathway. These results suggest that ucOCN was internalized in an intact form or as a bound form and also propose the possibility of the presence of new target proteins in the cell membranes and/or in the cytoplasm for interaction with ucOCN in C2C12 cells.

The endocrine paradigm implying that OCN activates a widely expressed G protein–coupled receptor, GPRC6A to exert its endocrine function is supported by recent reports [34]. Although class C GPCRs, also called "nutrient receptors," are activated by numerous ligands, some studies do not show consistency in osteocalcin activation by class C GPCRs, including GPRC6A. In Chinese hamster ovary (CHO) cells, osteocalcin did not activate the GPRC6A-mediated signaling pathway [65]. Jacobsen et al demonstrated the internalization and constitutive recycling of GPRC6A in CHO cells; however, these events were not directly associated with the ligand-mediated signaling pathway. In addition, Oury et al [66] reported that osteocalcin signaling is not specifically mediated by GPRC6A in Leydig cells. Importantly, previous results obtained with GPRC6A-deficient mouse models are not consistent with respect to GPRC6A mediated signaling in glucose homeostasis [32, 69]. In addition to GPRC6A, an orphan class C G protein–coupled receptor (GPCR) Gpr158, which is expressed in the neurons of the hippocampal CA3 region, has been introduced as another osteocalcin-sensing receptor. Khrimian et al [70] reported that Gpr158 mediates ucOCN-based regulation of cognitive function and memory. We also conducted studies to identify the ucOCN binding target protein concerning anti-inflammatory effect in myoblasts using biotin tag and liquid chromatography–tandem mass spectrometry (LC-MS/MS) methodology and found that GPR158 also is not an ucOCN-sensing receptor in myoblast (data not shown here). Further studies are required to identify additional osteocalcin-sensing receptors recognized by various cell types.

Interestingly, GPRC6A itself seems to regulate TNF-α–induced IL-1β expression, regardless of ucOCN treatment. TNF-α–induced IL-1β expression was inhibited by knockdown or deletion of GPRC6A.

Quandt et al have reported a significant decrease in Alum-induced IL-1β expression in GPRC6A$^{-/-}$ mice, suggesting that GPRC6A itself may mediate inflammatory signaling. However, the levels of IL-6 and TNF-α were not significantly affected, as demonstrated by ELISA [71]. Rossol et al demonstrated that extracellular Ca^{2+} acts as a signal that activates the NLRP3 inflammasome via GPRC6A. They also showed that under in vivo conditions, increased calcium concentrations can amplify the inflammatory response in a mouse model of carrageenan-induced footpad swelling. This effect was inhibited in GPRC6A$^{-/-}$ mice [72]. In the present study, the increase in TNF-α induced IL-1β expression was observed in the siGPRC6A group; however, the increment was not as high as that in the siCON group (5.8-fold vs 25.5-fold) (Fig. 5B). Moreover, in the group with GPRC6A receptor deficiency or deletion, a significant increase in TNF-α–induced IL-1β expression was not detected at the protein level. Since ucOCN (0.5 ng/mL) reduced the TNF-α-induced IL-1β expression to the control group baseline level, we could not confirm the additive or synergistic effect of GPRC6A in the ucOCN treatment group (Figs. 5C

and 6C). Beyond our results showing that GPRC6A is not the ucOCN-sensing receptor with respect to the ucOCN-mediated anti-inflammatory signaling pathway in C2C12 cells, further studies investigating the role of GPRA6A itself as an inflammatory mediator and the inhibition of GPRC6A as another anti-inflammatory mechanism is justified.

Besides the endocrine role of OCN in regulating glucose and energy metabolism and male fertility, ucOCN signaling also correlates with cognitive function and anxiety regulation in the brain. Previous studies have shown that ucOCN$^{-/-}$ adult mice frequently show a spatial cognitive decline, memory deficits, and anxiety behavior. The hippocampal area is smaller and the corpus islet area is often missing in ucOCN$^{-/-}$ adult mice. In addition, the acquisition of cognitive function and brain development of offspring is affected by maternal ucOCN [53, 54]. In ucOCN$^{-/-}$ mice, reduced accumulation of dopamine, norepinephrine, and serotonin and increased accumulation of γ-aminobutyric acid have been observed in both the midbrain and brainstem [52]. With respect to ucOCN-mediated regulation of glucose and energy metabolism in muscles, Mera et al reported that chronically administered ucOCN improves the exercise capacity of young mice (3-month-old mice) and restores the exercise capacity in older mice (15-month-old mice) compared with that of young mice [68]. These results demonstrate that ucOCN plays a role in the muscle fibers, promoting the uptake and utilization of glucose and fatty acids, which contribute to muscle adaptation during exercise. Beyond this regulatory role in muscle energy metabolism, our study provides insights into the role of ucOCN in the inflammatory response in myoblastic cells.

In summary, circulating ucOCN suppressed inflammatory factor expression via the inhibition of the TNF-α–mediated downstream signaling pathway. GPRC6A did not mediate the ucOCN inflammation-regulating signaling pathway in C2C12 cells. This result is indicative of another endocrine and physiological role of the skeletal system. The results of the present study could be applied for the development of novel, bio-derived molecule-based drugs that mitigate the expression of various musculoskeletal inflammatory factors.

Disclosures

None.

Data Availability

Original data generated and analyzed during this study are included in this published article or in the data repositories listed in References.

References

1. Hauschka PV, Lian JB, Cole DE, Gundberg CM. Osteocalcin and matrix Gla protein: vitamin K-dependent proteins in bone. *Physiol Rev.* 1989;69(3):990-1047. doi:10.1152/physrev.1989.69.3.990

2. Hauschka PV, Wians FH Jr. Osteocalcin-hydroxyapatite interaction in the extracellular organic matrix of bone. *Anat Rec.* 1989;224(2):180-188. doi:10.1002/ar.1092240208

3. Stafford DW. The vitamin K cycle. *J Thromb Haemost.* 2005;3(8):1873-1878. doi:10.1111/j.1538-7836.2005.01419.x

4. Dowd TL, Rosen JF, Li L, Gundberg CM. The three-dimensional structure of bovine calcium ion-bound osteocalcin using 1H NMR spectroscopy. *Biochemistry.* 2003;42(25):7769-7779. doi:10.1021/bi034470s

5. Ferron M, Wei J, Yoshizawa T, et al. Insulin signaling in osteoblasts integrates bone remodeling and energy metabolism. *Cell.* 2010;142(2):296-308. doi:10.1016/j.cell.2010.06.003

6. Cairns JR, Price PA. Direct demonstration that the vitamin K-dependent bone Gla protein is incompletely gamma-carboxylated in humans. *J Bone Miner Res.* 1994;9(12):1989-1997. doi:10.1002/jbmr.5650091220

7. Ferron M, Wei J, Yoshizawa T, Ducy P, Karsenty G. An ELISA-based method to quantify osteocalcin carboxylation in mice. *Biochem Biophys Res Commun.* 2010;397(4):691-696. doi:10.1016/j.bbrc.2010.06.008

8. Gundberg CM, Lian JB, Booth SL. Vitamin K-dependent carboxylation of osteocalcin: friend or foe? *Adv Nutr.* 2012;3(2):149-157. doi:10.3945/an.112.001834

9. Harada S, Rodan GA. Control of osteoblast function and regulation of bone mass. *Nature.* 2003;423(6937):349-355. doi:10.1038/nature01660

10. Lee AJ, Hodges S, Eastell R. Measurement of osteocalcin. *Ann Clin Biochem.* 2000;37(Pt 4):432-446. doi:10.1177/000456320003700402

11. Plantalech L, Guillaumont M, Vergnaud P, Leclercq M, Delmas PD. Impairment of gamma carboxylation of circulating osteocalcin (bone gla protein) in elderly women. *J Bone Miner Res.* 1991;6(11):1211-1216. doi:10.1002/jbmr.5650061111

12. Schilling AF, Schinke T, Munch C, et al. Increased bone formation in mice lacking apolipoprotein E. *J Bone Miner Res.* 2005;20(2):274-282. doi:10.1359/JBMR.041101

13. Vergnaud P, Garnero P, Meunier PJ, Breart G, Kamihagi K, Delmas PD. Undercarboxylated osteocalcin measured with a specific immunoassay predicts hip fracture in elderly women: the EPIDOS Study. *J Clin Endocrinol Metab.* 1997;82(3):719-724. doi:10.1210/jcem.82.3.3805

14. Biolo G, Cederholm T, Muscaritoli M. Muscle contractile and metabolic dysfunction is a common feature of sarcopenia of aging and chronic diseases: from sarcopenic obesity to cachexia. *Clin Nutr.* 2014;33(5):737-748. doi:10.1016/j.clnu.2014.03.007

15. Muscaritoli M, Anker SD, Argiles J, et al. Consensus definition of sarcopenia, cachexia and pre-cachexia: joint document elaborated by Special Interest Groups (SIG) "cachexia-anorexia in chronic wasting diseases" and "nutrition in geriatrics". *Clin Nutr.* 2010;29(2):154-159. doi:10.1016/j.clnu.2009.12.004

16. Costelli P, Baccino FM. Mechanisms of skeletal muscle depletion in wasting syndromes: role of ATP-ubiquitin-dependent proteolysis. *Curr Opin Clin Nutr Metab Care.* 2003;6(4):407-412. doi:10.1097/01.mco.0000078984.18774.02

17. Du J, Wang X, Miereles C, et al. Activation of caspase-3 is an initial step triggering accelerated muscle proteolysis in catabolic conditions. *J Clin Invest.* 2004;113(1):115-123. doi:10.1172/JCI18330

18. Hasselgren PO, Wray C, Mammen J. Molecular regulation of muscle cachexia: it may be more than the proteasome. *Biochem Biophys Res Commun.* 2002;290(1):1-10. doi:10.1006/bbrc.2001.5849

19. Penna F, Baccino FM, Costelli P. Coming back: autophagy in cachexia. *Curr Opin Clin Nutr Metab Care.* 2014;17(3):241-246. doi:10.1097/MCO.0000000000000048

20. Carnio S, LoVerso F, Baraibar MA, et al. Autophagy impairment in muscle induces neuromuscular junction degeneration and precocious aging. *Cell Rep.* 2014;8(5):1509-1521. doi:10.1016/j.celrep.2014.07.061

21. Molanouri Shamsi M, Hassan ZH, Gharakhanlou R, et al. Expression of interleukin-15 and inflammatory cytokines in skeletal muscles of STZ-induced diabetic rats: effect of resistance exercise training. *Endocrine.* 2014;46(1):60-69. doi:10.1007/s12020-013-0038-4

22. Lee JS, Auyeung TW, Kwok T, Lau EM, Leung PC, Woo J. Associated factors and health impact of sarcopenia in older Chinese men and women: a cross-sectional study. *Gerontology.* 2007;53(6):404-410. doi:10.1159/000107355

23. Reed SA, LaVigne EK, Jones AK, Patterson DF, Schauer AL. Horse species symposium: the aging horse: effects of inflammation on muscle satellite cells. *J Anim Sci.* 2015;93(3):862-870. doi:10.2527/jas.2014-8448

24. Ye J, Zhang Y, Xu J, Zhang Q, Zhu D. FBXO40, a gene encoding a novel muscle-specific F-box protein, is upregulated in denervation-related muscle atrophy. *Gene* 2007;404(1-2):53-60. doi:10.1016/j.gene.2007.08.020

25. Shi J, Luo L, Eash J, Ibebunjo C, Glass DJ. The SCF-Fbxo40 complex induces IRS1 ubiquitination in skeletal muscle, limiting IGF1 signaling. *Dev Cell.* 2011;21(5):835-847. doi:10.1016/j.devcel.2011.09.011

26. Bador KM, Wee LD, Halim SA, et al. Serum osteocalcin in subjects with metabolic syndrome and central obesity. *Diabetes Metab Syndr.* Jan-Mar 2016;10(1 Suppl 1):S42-5. doi:10.1016/j.dsx.2015.09.009

27. Bal A, Unlu E, Bahar G, Aydog E, Eksioglu E, Yorgancioglu R. Comparison of serum IL-1 beta, sIL-2R, IL-6, and TNF-alpha levels with disease activity parameters in ankylosing spondylitis. *Clin Rheumatol.* 2007;26(2):211-215. doi:10.1007/s10067-006-0283-5

28. Franck H, Keck E. Serum osteocalcin and vitamin D metabolites in patients with ankylosing spondylitis. *Ann Rheum Dis.* 1993;52(5):343-346. doi:10.1136/ard.52.5.343

29. Naser A, Odeh AK, Sharp RC, Qasem A, Beg S, Naser SA. Polymorphisms in TNF receptor superfamily 1B (TNFRSF1B:rs3397) are linked to Mycobacterium avium paratuberculosis infection and osteoporosis in rheumatoid arthritis. *Microorganisms.* 2019;7(12):646. doi:10.3390/microorganisms7120646

30. Yasumura S, Aloia JF, Gundberg CM, et al. Serum osteocalcin and total body calcium in normal pre- and postmenopausal women and postmenopausal osteoporotic patients. *J Clin Endocrinol Metab.* 1987;64(4):681-685. doi:10.1210/jcem-64-4-681

31. Oury F, Sumara G, Sumara O, et al. Endocrine regulation of male fertility by the skeleton. *Cell.* 2011;144(5):796-809. doi:10.1016/j.cell.2011.02.004

32. Pi M, Chen L, Huang MZ, et al. GPRC6A null mice exhibit osteopenia, feminization and metabolic syndrome. *PLoS One.* 2008;3(12):e3858. doi:10.1371/journal.pone.0003858

33. Pi M, Quarles LD. Multiligand specificity and wide tissue expression of GPRC6A reveals new endocrine networks. *Endocrinology.* 2012;153(5):2062-2069. doi:10.1210/en.2011-2117

34. Pi M, Kapoor K, Ye R, et al. Evidence for Osteocalcin Binding and Activation of GPRC6A in beta-Cells. *Endocrinology.* 2016;157(5):1866-1880. doi:10.1210/en.2015-2010

35. Wei J, Hanna T, Suda N, Karsenty G, Ducy P. Osteocalcin promotes beta-cell proliferation during development and adulthood through GPRC6A. *Diabetes.* 2014;63(3):1021-1031. doi:10.2337/db13-0887

36. Park D, Gu H, Baek JH, Baek K. Undercarboxylated osteocalcin downregulates pancreatic lipase expression in an ATF4-dependent manner in pancreatic acinar cells. *Bone.* 2019;127:220-227. doi:10.1016/j.bone.2019.06.009

37. Liu S, Gao F, Wen L, et al. Osteocalcin induces proliferation via positive activation of the PI3K/Akt, P38 MAPK pathways and promotes differentiation through activation of the GPRC6A-ERK1/2 pathway

in C2C12 myoblast cells. *Cell Physiol Biochem.* 2017;43(3):1100-1112. doi:10.1159/000481752

38. Harno E, Edwards G, Geraghty AR, *et al.* Evidence for the presence of GPRC6A receptors in rat mesenteric arteries. *Cell Calcium.* 2008;44(2):210-219. doi:10.1016/j.ceca.2007.11.011

39. Hovatta I, Zapala MA, Broide RS, *et al.* DNA variation and brain region-specific expression profiles exhibit different relationships between inbred mouse strains: implications for eQTL mapping studies. *Genome Biol.* 2007;8(2):R25. doi:10.1186/gb-2007-8-2-r25

40. Kuang D, Yao Y, Lam J, Tsushima RG, Hampson DR. Cloning and characterization of a family C orphan G-protein coupled receptor. *J Neurochem.* 2005;93(2):383-391. doi:10.1111/j.1471-4159.2005.03025.x

41. Pi M, Faber P, Ekema G, *et al.* Identification of a novel extracellular cation-sensing G-protein-coupled receptor. *J Biol Chem.* 2005;280(48):40201-40209. doi:10.1074/jbc.M505186200

42. Wellendorph P, Brauner-Osborne H. Molecular cloning, expression, and sequence analysis of GPRC6A, a novel family C G-protein-coupled receptor. *Gene.* 2004;335:37-46. doi:10.1016/j.gene.2004.03.003

43. Pi M, Kapoor K, Wu Y, *et al.* Structural and Functional Evidence for Testosterone Activation of GPRC6A in Peripheral Tissues. *Mol Endocrinol.* 2015;29(12):1759-1773. doi:10.1210/me.2015-1161.

44. De Toni L, De Filippis V, Tescari S, *et al.* Uncarboxylated osteocalcin stimulates 25-hydroxy vitamin D production in Leydig cell line through a GPRC6a-dependent pathway. *Endocrinology.* 2014;155(11):4266-4274. doi:10.1210/en.2014-1283

45. Shahini A, Vydiam K, Choudhury D, *et al.* Efficient and high yield isolation of myoblasts from skeletal muscle. *Stem Cell Res.* 2018;30:122-129. doi:10.1016/j.scr.2018.05.017

46. Soriano-Arroquia A, Clegg PD, Molloy AP, Goljanek-Whysall K. Preparation and culture of myogenic precursor cells/primary myoblasts from skeletal muscle of adult and aged humans. *J Vis Exp.* 2017;(120):55047. doi:10.3791/55047

47. Park DK, Byun MR, Hwang HR, Ko SH, Baek JH, Baek K. Data from: Undercarboxylated, but not carboxylated, Osteocalcin (ucOCN) suppresses TNF-α induced inflammatory signaling pathway: GPRC6A does not mediate ucOCN anti-inflammatory signaling pathway in myoblasts. *Korea Research Data platform, DataOn.* 2022. doi:10.22711/idr/932. Deposited March 22, 2018. https://dataon.kisti.re.kr/search/view.do?drId=5fb8ae94-2cc9-446b-85c5-e82869229510

48. Sanjana NE, Shalem O, Zhang F. Improved vectors and genome-wide libraries for CRISPR screening. *Nat Methods.* 2014;11(8):783-784. doi:10.1038/nmeth.3047

49. Pi M, Wu Y, Lenchik NI, Gerling I, Quarles LD. GPRC6A mediates the effects of L-arginine on insulin secretion in mouse pancreatic islets. *Endocrinology.* 2012;153(10):4608-4615. doi:10.1210/en.2012-1301

50. Kanazawa I, Tanaka S, Sugimoto T. The association between osteocalcin and chronic inflammation in patients with type 2 diabetes mellitus. *Calcif Tissue Int.* 2018;103(6):599-605. doi:10.1007/s00223-018-0460-y

51. Sanchez-Enriquez S, Ballesteros-Gonzalez IT, Villafan-Bernal JR, *et al.* Serum levels of undercarboxylated osteocalcin are related to cardiovascular risk factors in patients with type 2 diabetes mellitus and healthy subjects. *World J Diabetes.* 2017;8(1):11-17. doi:10.4239/wjd.v8.i1.11

52. Ende G. Proton magnetic resonance spectroscopy: relevance of glutamate and GABA to neuropsychology. *Neuropsychol Rev.* 2015;25(3):315-325. doi:10.1007/s11065-015-9295-8

53. Oury F, Khrimian L, Denny CA, *et al.* Maternal and offspring pools of osteocalcin influence brain development and functions. *Cell.* 2013;155(1):228-241. doi:10.1016/j.cell.2013.08.042

54. Valenstein E, Bowers D, Verfaellie M, Heilman KM, Day A, Watson RT. Retrosplenial amnesia. *Brain.* 1987;110(Pt 6):1631-1646. doi:10.1093/brain/110.6.1631

55. Nabel GJ, Verma IM. Proposed NF-kappa B/I kappa B family nomenclature. *Genes Dev.* 1993;7(11):2063. doi:10.1101/gad.7.11.2063

56. Davis S, Vanhoutte P, Pages C, Caboche J, Laroche S. The MAPK/ERK cascade targets both Elk-1 and cAMP response element-binding protein to control long-term potentiation-dependent gene expression in the dentate gyrus in vivo. *J Neurosci.* 2000;20(12):4563-4572.

57. Hayakawa J, Depatie C, Ohmichi M, Mercola D. The activation of c-Jun NH2-terminal kinase (JNK) by DNA-damaging agents serves to promote drug resistance via activating transcription factor 2 (ATF2)-dependent enhanced DNA repair. *J Biol Chem.* 2003;278(23):20582-20592. doi:10.1074/jbc.M210992200

58. Raingeaud J, Gupta S, Rogers JS, *et al.* Pro-inflammatory cytokines and environmental stress cause p38 mitogen-activated protein kinase activation by dual phosphorylation on tyrosine and threonine. *J Biol Chem.* 1995;270(13):7420-7426. doi:10.1074/jbc.270.13.7420

59. Fuchs SY, Dolan L, Davis RJ, Ronai Z. Phosphorylation-dependent targeting of c-Jun ubiquitination by Jun N-kinase. *Oncogene.* 1996;13(7):1531-1535.

60. Fuchs SY, Xie B, Adler V, Fried VA, Davis RJ, Ronai Z. c-Jun NH2-terminal kinases target the ubiquitination of their associated transcription factors. *J Biol Chem.* 1997;272(51):32163-32168. doi:10.1074/jbc.272.51.32163

61. Musti AM, Treier M, Bohmann D. Reduced ubiquitin-dependent degradation of c-Jun after phosphorylation by MAP kinases. *Science.* 1997;275(5298):400-402. doi:10.1126/science.275.5298.400

62. Whitmarsh AJ, Davis RJ. Transcription factor AP-1 regulation by mitogen-activated protein kinase signal transduction pathways. *J Mol Med (Berl).* 1996;74(10):589-607. doi:10.1007/s001090050063

63. Zhou B, Li H, Liu J, *et al.* Intermittent injections of osteocalcin reverse autophagic dysfunction and endoplasmic reticulum stress resulting from diet-induced obesity in the vascular tissue via the NFkappaB-p65-dependent mechanism. *Cell Cycle.* 2013;12(12):1901-1913. doi:10.4161/cc.24929

64. Pi M, Wu Y, Quarles LD. GPRC6A mediates responses to osteocalcin in beta-cells in vitro and pancreas in vivo. *J Bone Miner Res.* 2011;26(7):1680-1683. doi:10.1002/jbmr.390

65. Jacobsen SE, Norskov-Lauritsen L, Thomsen AR, *et al.* Delineation of the GPRC6A receptor signaling pathways using a mammalian cell line stably expressing the receptor. *J Pharmacol Exp Ther.* 2013;347(2):298-309. doi:10.1124/jpet.113.206276

66. Oury F, Sumara G, Sumara O, *et al.* Endocrine regulation of male fertility by the skeleton. *Cell.* 2011;144(5):796-809. doi:10.1016/j.cell.2011.02.004

67. Dreaden EC, Gryder BE, Austin LA, *et al.* Antiandrogen gold nanoparticles dual-target and overcome treatment resistance in hormone-insensitive prostate cancer cells. *Bioconjug Chem.* 2012;23(8):1507-1512. doi:10.1021/bc300158k

68. Mera P, Laue K, Ferron M, *et al.* Osteocalcin signaling in myofibers is necessary and sufficient for optimum adaptation to exercise. *Cell Metab.* 2016;23(6):1078-1092. doi:10.1016/j.cmet.2016.05.004

69. Smajilovic S, Clemmensen C, Johansen LD, *et al.* The L-alpha-amino acid receptor GPRC6A is expressed in the islets of Langerhans but is not involved in L-arginine-induced insulin release. *Amino Acids.* 2013;44(2):383-390. doi:10.1007/s00726-012-1341-8

70. Khrimian L, Obri A, Ramos-Brossier M, *et al.* Gpr158 mediates osteocalcin's regulation of cognition. *J Exp Med.* 2017;214(10):2859-2873. doi:10.1084/jem.20171320

71. Quandt D, Rothe K, Baerwald C, Rossol M. GPRC6A mediates Alum-induced Nlrp3 inflammasome activation but limits Th2 type antibody responses. *Sci Rep.* 2015;5:16719. doi:10.1038/srep16719

72. Rossol M, Pierer M, Raulien N, *et al.* Extracellular Ca2+ is a danger signal activating the NLRP3 inflammasome through G protein-coupled calcium sensing receptors. *Nat Commun.* 2012;3:1329. doi:10.1038/ncomms2339